# Where the electroweak phase transition ends

M. Gürtler*
*Institut für Theoretische Physik, Universität Leipzig, Germany*

E.-M. Ilgenfritz†
*Institut für Physik, Humboldt-Universität zu Berlin, Germany*

A. Schiller‡
*Institut für Theoretische Physik, Universität Leipzig, Germany*

(Received 24 April 1997; revised manuscript received 12 June 1997)

We give a more precise characterization of the end of the electroweak phase transition in the framework of the effective three-dimensional SU(2)-Higgs lattice model than has been given before. The model has now been simulated at gauge couplings $\beta_G=12$ and 16 for Higgs boson masses $M_H^*=70$, 74, 76, and 80 GeV up to lattices $96^3$ and the data have been used for reweighting. The breakdown of finite volume scaling of the Lee-Yang zeroes indicates the change from a first order transition to a crossover at $\lambda_3/g_3^2=0.102(2)$ in rough agreement with results of Karsch, Neuhaus, Patkós, and Rank at $\beta_G=9$ and smaller lattices. The infinite volume extrapolation of the discontinuity $\Delta\langle\phi^+\phi\rangle/g_3^2$ turns out to be zero at $\lambda_3/g_3^2=0.107(2)$ being an upper limit. We comment on the limitations of the second method. [S0556-2821(97)02719-7]

PACS number(s): 11.15.Ha, 11.10.Wx, 14.80.Bn

## I. INTRODUCTION

During the last couple of years, much effort has been invested to study the properties of the first order phase transition that the standard model was expected to undergo at high temperature (for reviews see [1]). The motivation was to explore the phenomenological viability of the generation of the baryon asymmetry of the universe (BAU) at this transition.

The perturbative evaluation of the phase transition is prevented by infrared divergences in the so-called symmetric phase. Lattice Monte Carlo studies of the four-dimensional SU(2)-Higgs boson theory [2,3] have been done so far for relatively large lattice spacings [neglecting the U(1) gauge group and the fermionic content of the theory]. Another approach is based on the concept of dimensional reduction [4]. One maps the theory (with or without fermions) onto a three-dimensional SU(2)-Higgs boson model containing all infrared problems of the full theory and can investigate this effective theory by Monte Carlo simulations [5–8] with much less effort. Later, the U(1) gauge group was included into this approach, too [9].

BAU generation at the phase transition of the standard model is ruled out already, and the primary interest has shifted to extensions of the standard model. Nevertheless, the standard variant remains interesting in order (i) to understand methods such as dimensional reduction, validity of perturbation theory, etc., in the realm of extremely weakly first order phase transitions and (ii) to understand in general terms the physics in the strongly coupled high temperature phase of gauge-matter systems.

The present paper belongs to the first group of studies. We try to shed light on the question for which Higgs boson mass the first order transition ceases to exist and what replaces it at slightly higher Higgs boson mass. Analytical work has already addressed this problem. In [10] it was claimed that the transition between the broken and the symmetric phase can only be of first order or a smooth crossover. Within the same average action approach it was made more precise later [11] that the first order transition ends at a Higgs boson mass of about 80 GeV and the transition is replaced by a unique strongly interacting phase. A similar conclusion has been drawn from a renormalization group study of the electroweak phase transition [12]. Analyzing gap equations a similar critical Higgs boson mass has been pointed out in Ref. [13].

Recently, three-dimensional (3D) Monte Carlo studies [14,8] have investigated the volume dependence of the susceptibility of the Higgs boson condensate. These studies gave support to the claim that the transition turns into a smooth crossover for large Higgs boson masses. An attempt to determine the value of the upper critical Higgs boson mass has been performed in [8]. It was based on an analysis of the volume dependence of the Lee-Yang zeros [15], but for a relatively large lattice spacing. The exploration of critical behavior in lattice gauge theories using Lee-Yang zeroes has become a frequently used tool nowadays. A good guide to the basic applications can be found in [16].

The only 4D study to determine the critical Higgs boson mass region was presented in [17], however, with a temporal extent of only $N_t=2$ and an exploratory scan of the Higgs boson self-coupling (corresponding to different Higgs boson masses). In our present study we use Monte Carlo simulations of the three-dimensional theory in order to find the critical Higgs boson mass, employing two different types of analysis. The first is simply to look for the Higgs boson mass where the jump of the scalar condensate (which is propor-

*Electronic address: guertler@tph204.physik.uni-leipzig.de
†Electronic address: ilgenfri@pha1.physik.hu-berlin.de
‡Electronic address: schiller@tph204.physik.uni-leipzig.de

 

tional to the latent heat) vanishes. The second method is based on an analysis of the Lee-Yang zeroes of the partition function, whose finite volume behavior changes with the character of the transition and is able to characterize the change of first order into crossover.

## II. THE MODEL AND NUMERICAL TECHNIQUES

The lattice 3D SU(2)-Higgs boson model is defined by the action

$$S=\beta_G\sum_p\left(1-\frac{1}{2}\mathrm{tr}U_p\right)-\beta_H\sum_{x,\alpha}E_{x,\alpha}+\sum_x[\rho_x^2+\beta_R(\rho_x^2-1)^2], \tag{2.1}$$

$$E_{x,\alpha}=\frac{1}{2}\mathrm{tr}(\Phi_x^+U_{x,\alpha}\Phi_{x+\alpha}) \tag{2.2}$$

(summed over plaquettes $p$, sites $x$, and directions $\alpha$), with the gauge coupling $\beta_G$, the lattice Higgs boson self-coupling $\beta_R$ and the hopping parameter $\beta_H$. The gauge fields are represented by unitary $2\times2$ link matrices $U_{x,\alpha}$ and the Higgs boson fields are written as $\Phi_x=\rho_xV_x$. $\rho_x^2=1/2\mathrm{tr}(\Phi_x^+\Phi_x)$ is the Higgs boson modulus squared, $V_x$ an element of the group SU(2), $U_p$ denotes the SU(2) plaquette matrix. For shortness, we characterize as in [7] the Higgs self-coupling by an approximate Higgs boson mass $M_H^*$ defined through

$$\beta_R=\frac{\lambda_3}{g_3^2}\frac{\beta_H^2}{\beta_G}=\frac{1}{8}\left(\frac{M_H^*}{80\ \mathrm{GeV}}\right)^2\frac{\beta_H^2}{\beta_G}, \tag{2.3}$$

where $\lambda_3$ and $g_3$ are the dimensionful quartic and gauge couplings of the corresponding $3D$ continuum model, respectively. Both couplings are renormalization group invariants. The 3D continuum model is furthermore characterized by the renormalized mass $m_3(g_3^2)$ taken at the scale $\mu_3=g_3^2$. To study the continuum limit of the lattice model at given $M_H^*$ (along the line of constants physics of the 3D continuum theory) one has to keep the coupling ratios $\lambda_3/g_3^2$ and $m_3(\mu_3=g_3^2)/g_3^2$ fixed.

Letting increase the gauge coupling $\beta_G$ at fixed $\lambda_3/g_3^2$ along the critical line dividing the high temperature and Higgs boson phase [$m_3(g_3^2)/g_3^2$ fixed and near to zero] permits us to perform the continuum limit according to the relation

$$\beta_G=\frac{4}{ag_3^2}. \tag{2.4}$$

We study the phase transition driven by the hopping parameter $\beta_H$. The Monte Carlo simulations were performed at $\beta_G=12$ and $\beta_G=16$ for different $M_H^*$, ranging from 70 to 80 GeV at several values of $\beta_H$ on cubic lattices of the size $L^3$ (see Table I for parameters and statistics). The simulations were performed at the DFG Quadrics computer QH2 in Bielefeld and on the CRAY-T90 of the HLRZ Jülich; some data were collected on a Q4 Quadrics in Jülich. For the update we used the same algorithm as described in [7] which combines Gaussian heat bath updates for the gauge and Higgs boson fields with several reflections for the fields to reduce the autocorrelations. All thermodynamical bulk quantities are measured after each such combined sweep. One combined sweep with bulk measurements takes 3.5 sec on a $96^3$ lattice on the QH2 parallel computer.

TABLE I. Statistics.

| $M_H^*$ | $\beta_G$ | $L$ | $\beta_H$ | sweeps | $M_H^*$ | $\beta_G$ | $L$ | $\beta_H$ | sweeps |
|---|---|---|---|---|---|---|---|---|---|
| 70 | 12 | 30 | 0.343480 | 30 000 | 74 | 12 | 64 | 0.343848 | 20 000 |
| 70 | 12 | 30 | 0.343540 | 50 000 | 74 | 12 | 64 | 0.343850 | 25 000 |
| 70 | 12 | 30 | 0.343600 | 40 000 | 74 | 12 | 64 | 0.343852 | 30 000 |
| 70 | 12 | 40 | 0.343540 | 20 000 | 74 | 12 | 80 | 0.3438486 | 40 000 |
| 70 | 12 | 40 | 0.343560 | 20 000 | 74 | 12 | 96 | 0.3438486 | 40 000 |
| 70 | 12 | 48 | 0.343440 | 75 000 | 76 | 12 | 30 | 0.343980 | 20 000 |
| 70 | 12 | 48 | 0.343520 | 40 000 | 76 | 12 | 30 | 0.344000 | 80 000 |
| 70 | 12 | 48 | 0.343540 | 80 000 | 76 | 12 | 30 | 0.344040 | 20 000 |
| 70 | 12 | 48 | 0.343544 | 120 000 | 76 | 12 | 40 | 0.343990 | 20 000 |
| 70 | 12 | 48 | 0.343546 | 20 000 | 76 | 12 | 40 | 0.344000 | 30 000 |
| 70 | 12 | 48 | 0.343548 | 120 000 | 76 | 12 | 40 | 0.344020 | 20 000 |
| 70 | 12 | 48 | 0.343560 | 40 000 | 76 | 12 | 48 | 0.343994 | 25 000 |
| 70 | 12 | 48 | 0.343580 | 110 000 | 76 | 12 | 48 | 0.344000 | 35 000 |
| 70 | 12 | 64 | 0.343546 | 90 000 | 76 | 12 | 48 | 0.344006 | 35 000 |
| 70 | 12 | 64 | 0.343548 | 120 000 | 76 | 12 | 48 | 0.344012 | 10 000 |
| 70 | 12 | 64 | 0.343549 | 20 000 | 76 | 12 | 64 | 0.344000 | 40 000 |
| 70 | 12 | 64 | 0.343550 | 100 000 | 76 | 12 | 64 | 0.344006 | 40 000 |
| 70 | 12 | 80 | 0.343546 | 40 000 | 76 | 12 | 80 | 0.344002 | 20 000 |
| 70 | 16 | 32 | 0.340780 | 40 000 | 76 | 12 | 80 | 0.344002 | 40 000 |
| 70 | 16 | 32 | 0.340800 | 40 000 | 76 | 12 | 80 | 0.344006 | 25 000 |
| 70 | 16 | 32 | 0.340820 | 40 000 | 76 | 16 | 32 | 0.341100 | 20 000 |
| 70 | 16 | 40 | 0.340780 | 40 000 | 76 | 16 | 32 | 0.341120 | 40 000 |
| 70 | 16 | 40 | 0.340800 | 100 000 | 76 | 16 | 32 | 0.341140 | 20 000 |
| 70 | 16 | 40 | 0.340820 | 40 000 | 76 | 16 | 40 | 0.341120 | 30 000 |
| 70 | 16 | 48 | 0.340700 | 45 000 | 76 | 16 | 40 | 0.341124 | 30 000 |
| 70 | 16 | 48 | 0.340780 | 45 000 | 76 | 16 | 40 | 0.341130 | 20 000 |
| 70 | 16 | 48 | 0.340800 | 90 000 | 76 | 16 | 48 | 0.341124 | 35 000 |
| 70 | 16 | 48 | 0.340820 | 45 000 | 76 | 16 | 48 | 0.341128 | 20 000 |
| 70 | 16 | 64 | 0.340796 | 40 000 | 76 | 16 | 64 | 0.341124 | 40 000 |
| 70 | 16 | 64 | 0.340800 | 80 000 | 76 | 16 | 64 | 0.341128 | 20 000 |
| 70 | 16 | 64 | 0.340804 | 40 000 | 76 | 16 | 80 | 0.341126 | 20 000 |
| 70 | 16 | 80 | 0.340802 | 30 000 | 76 | 16 | 80 | 0.341130 | 30 000 |
| 74 | 12 | 48 | 0.343850 | 40 000 | 80 | 16 | 80 | 0.341360 | 40 000 |

In the search for the phase transition the space averaged square of the Higgs boson modulus

$$\rho^2=\frac{1}{L^3}\sum_x\rho_x^2 \tag{2.5}$$

is used; $\langle\rho^2\rangle$ denotes averaging over the Monte Carlo measurements.

In our analysis we used the Ferrenberg-Swendsen method [18]. Note that at fixed $M_H^*$ (and $\beta_G$) the Higgs self-coupling $\beta_R$ is quadratic in $\beta_H$ [see Eq. (2.3)]. The reweighting has to be performed by histogramming in two parts of the action. The partition function is represented as

$$Z(L,\beta_H)=\int dS_1 dS_2 D_L(S_1,S_2)\exp[L^3(\beta_H S_1-\beta_H^2 S_2)], \tag{2.6}$$

$$S_1=3E_{\rm link}, \quad S_2=\frac{\lambda_3}{g_3^2\beta_G}(\rho^4-2\rho^2), \tag{2.7}$$

where the density of states $D_L(S_1,S_2)$ is approximated by the histogram produced by multihistogram reweighting of all available data for given $\beta_G$ and $L^3$ (see Table I). Having a good estimator of the density of states $D_L(S_1,S_2)$ from a sufficient number of simulation points we are able to interpolate in $\beta_H$ at fixed $M_H^*$ to localize the phase transition, interpolate in $M_H^*$ in order to find the critical Higgs boson mass, and extrapolate to complex $\beta_H$ to study Lee-Yang zeros.

Finally, all considered quantities are translated into physical units. This allows us to combine results obtained for different $\beta_G$ and gives a check to what extent the continuum limit is reached. The size of the lattice in continuum length units (i.e., the inverse 3D gauge coupling $g_3^2$) is given by the expression

$$lg_3^2=Lag_3^2=4L/\beta_G \tag{2.8}$$

and the jump of the quadratic scalar condensate is in the corresponding mass units

$$\frac{\Delta\langle\phi^+\phi\rangle}{g_3^2}=\frac{1}{8}\beta_G\beta_H\Delta\langle\rho^2\rangle. \tag{2.9}$$

Here $\Delta\langle\rho^2\rangle=\langle\rho_b^2\rangle-\langle\rho_s^2\rangle$ denotes the difference of the lattice quadratic scalar condensates measured at the pseudocritical hopping parameter between the broken ($\langle\rho_b^2\rangle$) and symmetric ($\langle\rho_s^2\rangle$) phases, respectively.

## III. THE BEHAVIOR OF THE LATENT HEAT WITH INCREASING HIGGS BOSON MASS

A nonvanishing latent heat $\Delta\epsilon$ is one of the characteristics for a first order phase transition. In our model the latent heat is proportional to the jump of the quadratic scalar condensate $\Delta\langle\phi^+\phi\rangle$ [5]. The proper identification of the scalar condensate discontinuity becomes increasingly demanding near to the end of the first order transition. The correlation length grows beyond the size of the system under study, in particular if the end point is a critical point. There can be an apparent metastability on a finite torus which delays the approach to the thermodynamical limit. In this section we identify the end of the phase transition with the point in the $\beta_H$–$M_H^*$ plane where the discontinuity vanishes.

The minimum of the Binder cumulant

$$B_{\rho^2}(L,\beta_H)=1-\frac{\langle(\rho^2)^4\rangle}{3\langle(\rho^2)^2\rangle^2} \tag{3.1}$$

and the maximum of the susceptibility of $\rho^2$

$$C_{\rho^2}(L,\beta_H)=\langle(\rho^2)^2\rangle-\langle\rho^2\rangle^2 \tag{3.2}$$

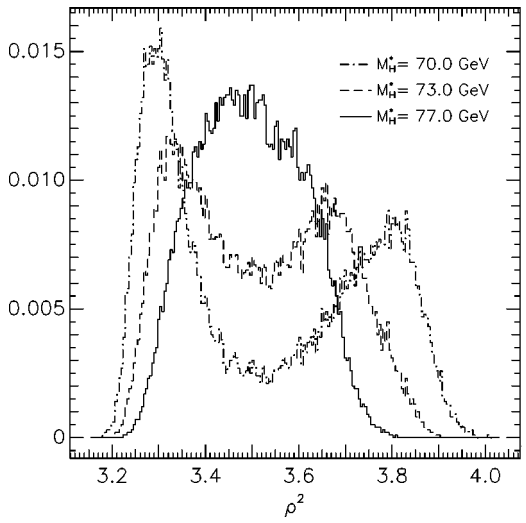


FIG. 1. Histograms of $\rho^2$ for different $M_H^*$ at the respective pseudocritical $\beta_H$ (defined by the minimum of the Binder cumulant) for a $80^3$ lattice, $\beta_G=12$.

are chosen to define pseudocritical values of the hopping parameter $\beta_H$. The jumps in $\Delta\langle\rho^2\rangle$ are extracted from the peaks of the histograms reweighted to these values of $\beta_H$. The $\rho^2$ histograms at the respective pseudocritical couplings show how the discontinuity decreases with increasing $M_H^*$. The gap between the peaks is more and more filled, and the distance between them becomes smaller (Fig. 1).

At any Higgs boson mass $M_H^*$ we attempt to perform the thermodynamical limit of $\Delta\langle\rho^2\rangle$ by assuming the finite size corrections to follow an inverse cross sectional law (suggested by the behavior of the Potts model in two dimensions [19]):

$$|\Delta\langle\phi^+\phi\rangle_\infty-\Delta\langle\phi^+\phi\rangle_l|\propto 1/l^2. \tag{3.3}$$

Figure 2 shows the different infinite volume extrapolation of $\Delta\langle\phi^+\phi\rangle/g_3^2$ at $M_H^*=70$ and 76 GeV. We have used two criteria (minimum of the Binder cumulant and maximum of

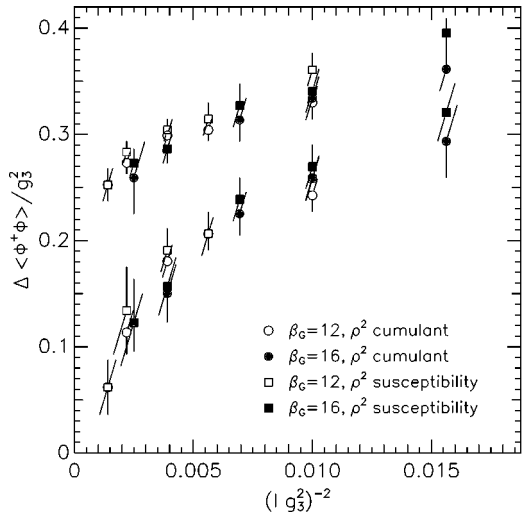


FIG. 2. Quadratic Higgs boson condensate jump $\Delta\langle\phi^+\phi\rangle/g_3^2$ as function of inverse physical length squared, upper data correspond to $M_H^*=70$ GeV, lower to $M_H^*=76$ GeV.

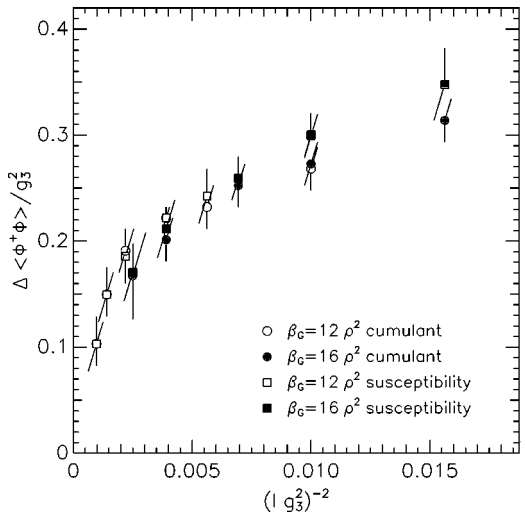


FIG. 3. Quadratic Higgs boson condensate jump $\Delta\langle\phi^+\phi\rangle/g_3^2$ as function of inverse physical length squared at $M_H^*=74$ GeV.

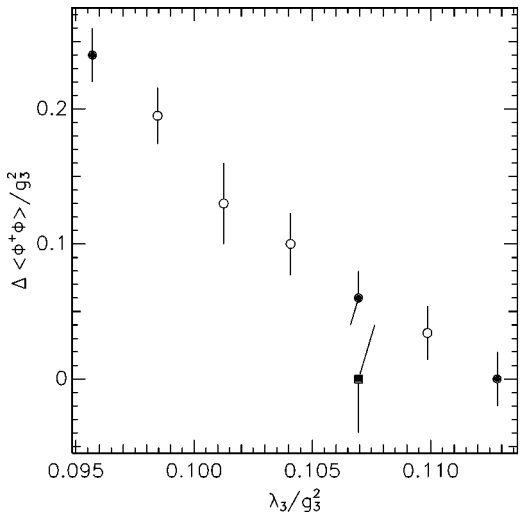


FIG. 4. Infinite volume discontinuity $\Delta\langle\phi^+\phi\rangle/g_3^2$ shown vs $\lambda_3/g_3^2$. Filled symbols mark the Higgs boson masses $M_H^*=70$, 74, and 76 GeV where data have been taken, open symbols denote results from FS interpolation. The isolated lower data point at $M_H^*=74$ GeV refers to an infinite volume extrapolation including only $80^3$ and $96^3$ lattices as described in the text.

the susceptibility for the lattice quadratic Higgs boson condensate) to determine the pseudocritical $\beta_H$. One observes that the data for different $\beta_G$ cluster along one curve within their errors and do not show a significant dependence on the lattice spacing $a$. Therefore, we conclude that the quadratic Higgs boson condensate jump at the measured $\beta_G$ values is already sufficiently near to the continuum limit. Obviously the latent heat at $M_H^*=76$ GeV has a vanishing thermodynamical limit. At the larger Higgs boson mass the assumed $1/l^2$ scaling compatible with the vanishing limit of the condensate sets in only for the largest considered volumes.

This feature becomes even more pronounced at intermediate Higgs boson mass $M_H^*=74$ GeV. Figure 3 shows the volume dependence of the condensate jump for $M_H^*=74$ GeV. This picture includes, besides reweighted data, original simulations at that Higgs boson mass for lattices up to $96^3$ at $\beta_G=12$. The onset of the $1/l^2$ scaling is delayed to lattices not smaller than $80^3$ (for $\beta_G=12$). If only those data are considered the latent heat is consistent with zero.

The summary of the extrapolations to the thermodynamical limit is collected in Fig. 4. For the extrapolation according to Eq. (3.3) we have used the results for the discontinuity at $(lg_3^2)^{-2}<0.003$ which correspond to lattices $\geqslant 64^3$ for $\beta_G=12$ and $80^3$ for $\beta_G=16$. For $\lambda_3/g_3^2\approx 0.107$ ($M_H^*=74$ GeV) a different extrapolation is shown, lying below the general trend, which is compatible with zero at that Higgs boson mass. This extrapolation takes into account only the two largest volumes at $\beta_G=12$. The uncertainty reflects the scattering of slopes of the straight line interpolation.

Concerning the two-parameter multihistogram extrapolation we can report that the purely interpolated histograms at $M_H=74$ GeV near to the end point are in reasonable agreement with histograms at that mass supported by actual simulations. However, at that mass we are too near to the endpoint, such that simulations at still larger lattices are necessary in order to estimate the correct thermodynamical limit.

We conclude that the critical coupling, if defined by vanishing latent heat (vanishing jump of the quadratic scalar condensate), is bounded from above as

$$\lambda_{3\ \mathrm{crit}}/g_3^2<0.107. \tag{3.4}$$

This bound is somewhat larger than the critical coupling given in [8]. It could be tempting to explain this difference to the somewhat smaller $\beta_G=9$ in their paper.

In this section we have assumed an early continuum limit by plotting data from different $\beta_G$ as a function of the physical lattice volume. The data were compatible with each other within the errors. The account for finite $a$ corrections of expectation values in the thermodynamical limit could be performed (if necessary) along the line of Ref. [20].

## IV. LEE-YANG ZEROES NEAR THE CRITICAL HIGGS BOSON MASS

In this section we will determine the critical Higgs boson mass by analyzing the position of the Lee-Yang zeroes in the complex $\beta_H$ plane and their motion with increasing size of the finite lattice system. Phase transitions correspond to nonanalytical behavior of the infinite volume free energy density as function of couplings which normally are real valued. This is signalled by zeroes in the complex plane (to which the relevant coupling constant is extended) of the partition function of finite systems. If there exists a phase transition driven by this coupling some of these zeroes cluster, in the thermodynamical limit, along lines that pinch the real axis. This prevents the analytic continuation along the real axis corresponding to that coupling.

We sketch here the motion of the most important zeros with increasing volume. Neglecting interface tension effects the partition function at the transition point is given by the contributions of the two phases

$$Z=Z_s+Z_b=e^{-L^3 f_s}+e^{-L^3 f_b}, \tag{4.1}$$

where $f_{s(b)}$ denotes the lattice free energy per site of the so-called symmetric (broken) phase. The free energy density can be expanded around the real-valued pseudocritical coupling $\beta_{Hc}$

$$f_{s,b}(\beta_H)=f(\beta_{Hc})+\langle E_{s,b}(\beta_{Hc})\rangle(\beta_H-\beta_{Hc}) + O[(\beta_H-\beta_{Hc})^2]. \quad (4.2)$$

To obtain $\langle E\rangle$ we use the action in the form

$$S=S_0-3\beta_H L^3 E_{\rm link}+\beta_R^2 L^3(\rho^4-2\rho^2), \quad (4.3)$$

with $\rho^2$ defined in Eq. (2.5) and

$$E_{\rm link}=\frac{1}{3L^3}\sum_{x,\alpha} E_{x,\alpha}, \quad \rho^4=\frac{1}{L^3}\sum_x \rho_x^4. \quad (4.4)$$

Taking into account that the Higgs boson self-coupling is (for given $M_H^*$) quadratic in $\beta_H$ we find

$$\langle E(\beta_{Hc})\rangle=-3\langle E_{\rm link}\rangle+2\frac{\beta_{Rc}}{\beta_{Hc}}(\langle\rho^4\rangle-2\langle\rho^2\rangle), \quad (4.5)$$

where $\langle\cdots\rangle$ denotes the Monte Carlo average as before.

Using the decomposition at $\beta_{Hc}$

$$\langle E_{s(b)}\rangle=\langle E\rangle\mp\frac{1}{2}\Delta\langle E\rangle, \quad (4.6)$$

the partition sum behaves as

$$Z\propto\cosh\left[\frac{\Delta\langle E\rangle}{2}L^3(\beta_H-\beta_{Hc})\right]. \quad (4.7)$$

For the complex coupling $\beta_H={\rm Re}\beta_H+i\ {\rm Im}\beta_H$ we obtain in this approximation that the zeroes of the complex partition function $Z$ are located at ($n$ are integers)

$${\rm Im}\beta_H^{(n)}=\frac{2\pi}{L^3|\Delta\langle E\rangle|}\left(n-\frac{1}{2}\right), \quad (4.8)$$

$${\rm Re}\beta_H=\beta_{Hc}. \quad (4.9)$$

For a volume independent $\Delta\langle E\rangle$ the imaginary part of the hopping parameter at the position of the zeroes would scale with the inverse volume. For infinite volume the zeroes become dense and prevent analytic continuation of $Z$ beyond $\beta_{Hc}$.

Taking into account Eq. (4.5) and using the identity for the condensate jumps [7]

$$-3\beta_{Hc}\ \Delta\langle E_{\rm link}\rangle+(1-2\beta_{Rc})\Delta\langle\rho^2\rangle+2\beta_{Rc}\ \Delta\langle\rho^4\rangle=0 \quad (4.10)$$

one easily finds

$$-\Delta\langle E\rangle=\frac{1+2\beta_{Rc}}{\beta_{Hc}}\Delta\langle\rho^2\rangle. \quad (4.11)$$

Therefore, for the phase transition still being first order one expects the approximate relation between the imaginary part of the leading zeros in the complex hopping parameter plane (with index $n$) and the Higgs boson condensate discontinuity

$${\rm Im}\beta_H^{(n)}=\frac{2\pi\beta_{Hc}}{L^3(1+2\beta_{Rc})\Delta\langle\rho^2\rangle}\left(n-\frac{1}{2}\right). \quad (4.12)$$

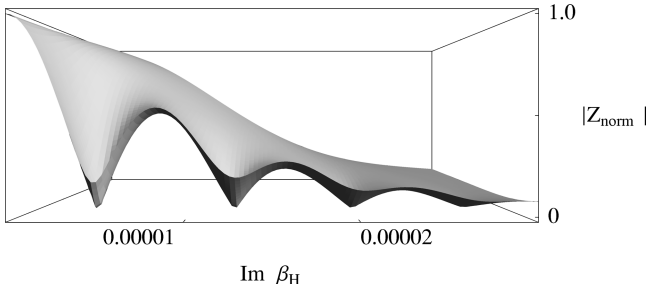


FIG. 5. 3D view of $|Z_{\rm norm}|$ near to the first zeroes at $\beta_G=12$, $80^3$ and $M_H^*=70$ GeV.

Since $\Delta\langle\rho^2\rangle$ itself depends on the size of the lattice (as discussed in Sec. III) the simple $1/L^3$ behavior for Im $\beta_H$ is modified and can be expected only asymptotically.

An analysis of the first Lee-Yang zero in the crossover region of the 3D SU(2)-Higgs boson model has been carried out recently in Ref. [8]. Here we are interested to discuss in more detail the change from first order transition to a crossover behavior at the critical Higgs boson mass.

As usual, the partition function has to be analytically continued into the complex plane as function of the complex hopping parameter $\beta_H$ near to the real pseudocritical coupling $\beta_{Hc}$. This can be done by reweighting using Eq. (2.6). Since $\beta_H$ is complex, the action $S$ and consequently $Z$ become complex, too. The zeroes of $Z$ are found numerically using the Newton-Raphson method for solving simultaneously ${\rm Re}Z=0$ and ${\rm Im}Z=0$. To estimate the accuracy of the position of the zeroes in the complex plane we have calculated them using only the half data sample.

In Fig. 5 the modulus of the complex partition function $|Z_{\rm norm}|$ in the neighborhood of the pseudocritical hopping parameter $\beta_{Hc}$ is shown. $Z_{\rm norm}$ has been used for clarity. This means that $Z(\beta_H)$ is divided, for each complex $\beta_H$, by its (real) value at ${\rm Re}\beta_H$, $Z({\rm Re}\beta_H)$. The figure represents a lattice of size $80^3$ at $\beta_G=12$ for a Higgs boson mass $M_H^*=70$ GeV, where the transition is still clearly first order [7]. The normalized $|Z_{\rm norm}|$ approaches zero in the clearly distinct minima.

The difference in the pattern of the leading complex zeroes is demonstrated in Figs. 6 and 7 referring to $M_H^*=70$ and 76 GeV for the same lattice size $80^3$ and lattice gauge coupling $\beta_G=12$. Each figure shows a part of the strip $0\leq{\rm Im}\beta_H\leq 3\times10^{-4}$ along the real axis where the leading Lee-Yang zeroes are located at the respective Higgs boson mass. For the larger Higgs boson mass the normalized modulus decreases much faster with increasing ${\rm Im}\beta_H$, less zeroes are localized inside the strip and the funnels which form the $|Z_{\rm norm}|$ landscape at the locations of the Lee-Yang zeros become less steep. The zeros move away from the real axis with increasing Higgs boson mass. Notice that only for the lower Higgs boson mass the pattern approximately follows

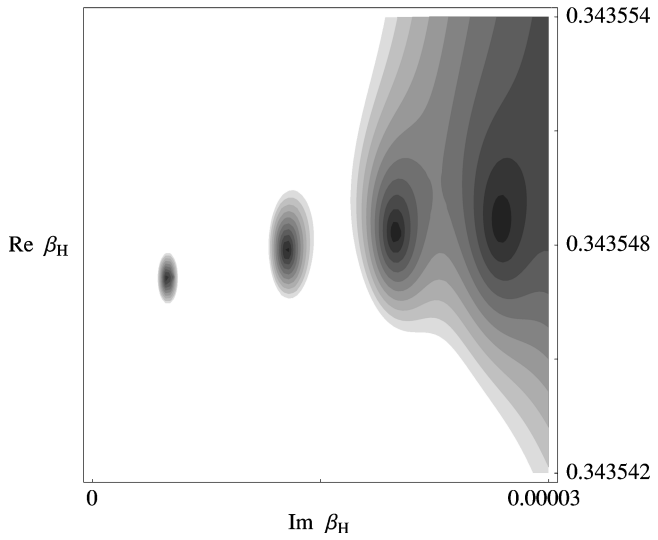


FIG. 6. Contour plot of $|Z_{\mathrm{norm}}|$ below 0.2 at $\beta_G=12$, $80^3$ and $M_H^*=70$ GeV with height differences of 0.02.

the $n$ dependence given in Eq. (4.12). This is a hint for an inherently different behavior of the model at these selected Higgs boson masses. To answer the question whether this difference shows the vanishing of the phase transition we investigate the zeroes in the thermodynamical limit.

In Fig. 8 the first two zeros of different lattice volumes are collected. There is a tendency of the zeros to move to larger $\mathrm{Re}\beta_H$ with decreasing lattice volume and increasing index of the zero (for low $n$). The first tendency corresponds with the fact that the maximum of the link susceptibility gives a pseudocritical $\beta_H$ which approaches the infinite volume limit $\beta_{Hc}$ from above [7].

To extract information about the end point of the transition we fit the imaginary part of the first zero for each available physical length $l$ [Eq. (2.8)] according to

$$\mathrm{Im}\beta_H^{(1)}=C(lg_3^2)^{-\nu}+R. \tag{4.13}$$

A positive $R$ in Eq. (4.13) should indicate that the first zero does not approach anymore the real axis in the thermodynamical limit (as required for a phase transition) and our first order transition has turned into a crossover.

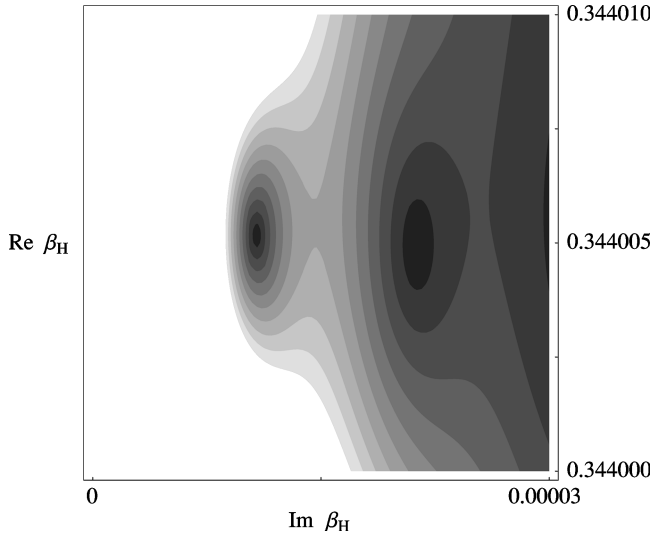


FIG. 7. Same as Fig. 6 at $\beta_G=12$, $80^3$ and $M_H^*=76$ GeV.

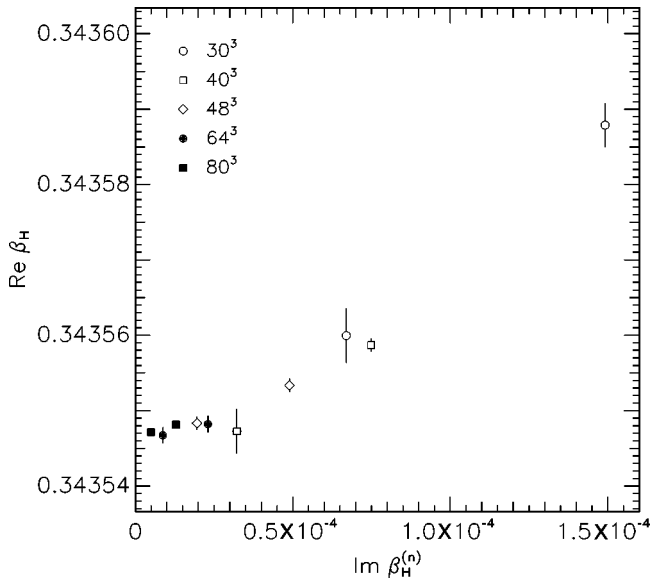


FIG. 8. First two zeroes at $\beta_G=12$ and $M_H^*=70$ GeV for different lattice sizes.

We assume that for equal physical volume the imaginary part of the Lee-Yang zeros shows a universal behavior. The values of $\ln\mathrm{Im}\beta_H^{(1)}$ are shifted to

$$\ln\ \mathrm{Im}\beta_H^{(1)}\rightarrow\ln\ \mathrm{Im}\beta_H^{(1)}-\ln(c_1c_2) \tag{4.14}$$

in order to use the results of both gauge couplings for the fit (Fig. 9). The main shift $\ln c_1$ is derived from Eq. (4.12) assuming that the continuum condensate jump is already independent of $a$:

$$c_1=\frac{\beta_{Hc}^2}{\beta_G^2(1+2\beta_{Rc})}. \tag{4.15}$$

In the logarithmic shift we have used the real-valued finite volume couplings $\mathrm{Re}\beta_H^{(1)}$ and $\beta_R(\mathrm{Re}\beta_H^{(1)})$. A small extra shift $\ln c_2$ (with $c_2$ between 1.028 and 1.095 in the used range of $\lambda_3/g_3^2$) has been added to correct the eventual imprecision of the used equation. It has been adjusted in a way to provide a minimal $\chi^2$ for all (reweighted) data at given $\lambda_3/g_3^2$ in the fit of Eq. (4.13). The three right-most data points in Fig. 9 arises from $96^3$ data at $M_H^*=74$ GeV which are reweighted to $M_H^*=72$ and 76 GeV, too.

The values of the fit constant $R$ using all lattice sizes and both gauge couplings at fixed $\lambda_3/g_3^2$ are given in Fig. 10. Near to the end point the $\chi^2$ of the fits deteriorate. For smaller lattice sizes the asymptotic behavior $\propto 1/l^3$ of $\mathrm{Im}\beta_H^{(1)}$ is still not reached. Hence the constant $R$ is found negative as long as the phase transition is of first order. We localize the end point of the transition where $R$ as a function of $\lambda_3/g_3^2$ crosses zero. This gives the critical value

$$\lambda_{3\ \mathrm{crit}}/g_3^2=0.102(2), \tag{4.16}$$

which translates into $M_{H\ \mathrm{crit}}^*=72.2(6)$ GeV.

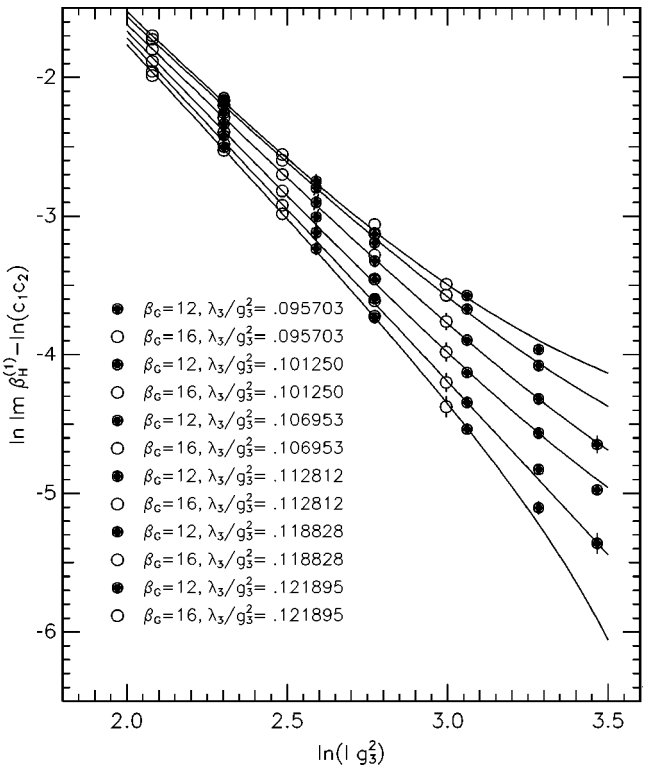


FIG. 9. Logarithm of the imaginary part of first zeroes at different $\lambda_3/g_3^2$ vs logarithm of the physical length $\ln(lg_3^2)$ together with the fit described in the text.

Restricting the fit of Eq. (4.13) only to larger volumes the expected power $\nu=3$ for the first order transition is reproduced. This is shown in Fig. 11 where only six (seven) data points above $\ln(lg_3^2)=2.55$ (see Fig. 9) are included in the fit. For $\lambda_3/g_3^2>0.102$ the fit yields a power which strongly decreases. This again indicates the change to the crossover. This critical Higgs boson coupling is only slightly below the upper bound obtained in Sec. III from the argument of vanishing latent heat.

## V. DISCUSSION AND CONCLUSIONS

We have compared two methods which promised to give estimates for the critical Higgs boson mass. We have used on one hand a criterion based on the thermodynamical limit of

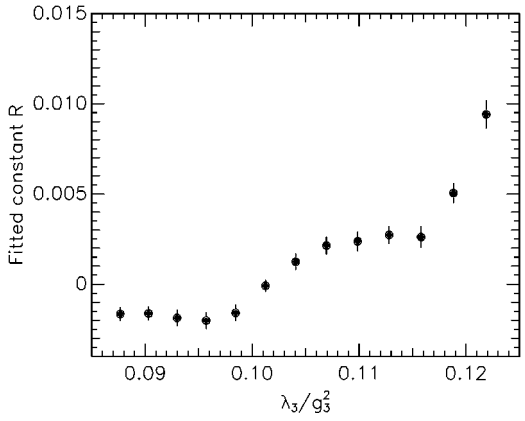


FIG. 10. Fitted distance $R$ as function of $\lambda_3/g_3^2$.

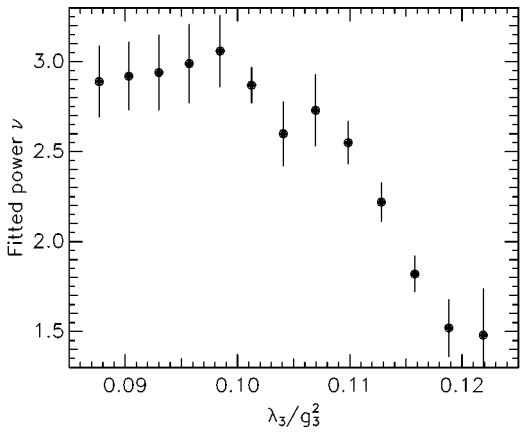


FIG. 11. Fitted power $\nu$ as function of $\lambda_3/g_3^2$.

Lee-Yang zeros, requiring that the leading zero approach the real axis in the infinite volume limit. This has led to the critical coupling ratio of Eq. (4.16). For this purpose we had to rescale results obtained with different values of the lattice gauge coupling, in our work $\beta_G=12$ and $\beta_G=16$.

The criterion based on a vanishing scalar condensate tends to predict a too high critical Higgs boson mass in accordance with the multihistogram interpolation. Very near to the end point a two-state signal persists which is not related to a first order phase transition. One has to use essentially larger lattices in order to get a reliable infinite volume extrapolation. By this technique we have identified the upper bound of Eq. (3.4).

The critical temperature $T_c$ and the actual Higgs boson mass $m_H$ of the underlying $4D$ theory corresponding to the endpoint of the first order transition can be calculated using the relations in Sec. II of [7]. These quantities are listed in Table II using the lattice couplings $\beta_G=12$ and $\beta_{Hc}=0.3437161$ at the critical continuum coupling ratio [Eq. (4.16)] as derived from the Lee-Yang zeroes analysis. Additionally, the four-dimensional $\overline{\text{MS}}$ running coupling $g^2(m_W)$ is given. All quantities are calculated for the two cases of the 4D SU(2)-Higgs boson theory, without fermions and including the top quark.

The apparent two-state signal for $\rho^2$ near or at the end point is misleading and cannot be an indicator of a first order phase transition. The reason is that the correlation length grows to the size of the system being simulated. At $M_H^*=70$ GeV, for instance, these two scales can be safely separated from each other [7]. When the transition becomes increasingly weak the situation will change rapidly. In order to measure the correlation length of the competing phases one would have to take some care. One should carefully monitor the tunneling of the system in order to measure the correlation functions of the pure phases, respectively. We have successfully applied such a procedure at $M_H^*=70$ GeV. For the

TABLE II. Some quantities at $\lambda_{3\,\text{crit}}/g_3^2=0.102$ ($M_{H\text{crit}}^*=72.2$ GeV); upper row without fermions, lower including top quarks.

| $m_H$/GeV | $T_c$/GeV | $g^2(m_W)$ |
|---|---|---|
| 67.0(8) | 154.8(2.6) | 0.423 |
| 72.4(9) | 110.0(1.5) | 0.429 |

weaker transitions at higher Higgs boson mass this becomes increasingly difficult. Therefore we have restricted our attention exclusively to bulk variables. At the critical endpoint one expects the correlation length to diverge.

Our result for $\lambda_{3\,\mathrm{crit}}/g_3^2$ is not so far from the result by Karsch *et al.* [8] who have obtained (in our notation)

$$\lambda_{3\,\mathrm{crit}}/g_3^2 = 0.0951(16), \tag{5.1}$$

at $\beta_G = 9$ analyzing lattices with an extent $\ln(lg_3^2) \leqslant 3.06$. The remaining difference between Eqs. (5.1) and (4.16) can comfortably be explained by the fact that we come nearer to the continuum limit.

It might be instructive to transform our results to a 4D SU(2)-Higgs model at a larger $\overline{\mathrm{MS}}$ running gauge coupling. Usually in 4D simulations, the bare coupling $g^2 = 0.5$ is used. The measured renormalized 4D gauge coupling does not seem to change significantly with the Higgs boson mass in the so far reported region from 18 to 49 GeV [3,21] and varies from 0.56 to 0.59. We expect that this coupling remains within this range at larger Higgs boson mass, too. Since a perturbative calculation is missing we assume here, following Refs. [22,23], that the measured renormalized gauge coupling roughly corresponds to the $\overline{\mathrm{MS}}$ running coupling.

For definiteness we choose $g^2(m_W) = 0.58$ and take $\lambda_3/g_3^2 = 0.102$. We obtain the critical Higgs boson mass $m_H = 65.2$ GeV and the corresponding transition temperature $T_c = 129.6$ GeV. This is noticeably smaller than the critical Higgs boson mass estimated in Ref. [17] which is the only 4D result so far available.

At weakly first order transitions, the 3D effective theory seems to describe the transition parameters of the 4D model reasonably well [22,23]. Concerning the apparent first order nature of the transition at $m_H \geqslant 67$ GeV in the 4D approach, there is reason for doubts because of the very coarse discretization with $N_t = 2$ temporal steps.

## ACKNOWLEDGMENTS

E.M.I. was supported by the DFG under Grant No. Mu932/3-4. The use of the DFG Quadrics QH2 parallel computer in Bielefeld and the Q4 parallel computer in the HLRZ Jülich is acknowledged. Additionally, we thank the council of HLRZ Jülich for providing CRAY-T90 resources. M.G. and A.S. are grateful to C. Borgs for a discussion about Lee-Yang zeros.

[1] K. Kajantie, Nucl. Phys. B (Proc. Suppl.) **42**, 103 (1995); K. Jansen, *ibid.* **47**, 196 (1996); K. Rummukainen, *ibid.* **53**, 30 (1997).
[2] B. Bunk, E.-M. Ilgenfritz, J. Kripfganz, and A. Schiller, Phys. Lett. B **284**, 371 (1992); Nucl. Phys. **B403**, 112 (1993).
[3] F. Csikor, Z. Fodor, J. Hein, and J. Heitger, Phys. Lett. B **357**, 156 (1995); Z. Fodor, J. Hein, K. Jansen, A. Jaster, and I. Montvay, Nucl. Phys. **B439**, 147 (1995); F. Csikor, Z. Fodor, J. Hein, A. Jaster, and I. Montvay, *ibid.* **B474**, 421 (1996).
[4] K. Farakos, K. Kajantie, K. Rummukainen, and M. Shaposhnikov, Nucl. Phys. **B425**, 67 (1994); K. Kajantie, M. Laine, K. Rummukainen, and M. Shaposhnikov, *ibid.* **B458**, 90 (1996).
[5] K. Kajantie, M. Laine, K. Rummukainen, and M. Shaposhnikov, Nucl. Phys. **B466**, 189 (1996).
[6] E.-M. Ilgenfritz, J. Kripfganz, H. Perlt, and A. Schiller, Phys. Lett. B **356**, 561 (1995).
[7] M. Gürtler, E.-M. Ilgenfritz, J. Kripfganz, H. Perlt, and A. Schiller, Nucl. Phys. **B483**, 383 (1997).
[8] F. Karsch, T. Neuhaus, A. Patkós, and J. Rank, Nucl. Phys. B (Proc. Suppl.) **53**, 623 (1997).
[9] K. Kajantie, M. Laine, K. Rummukainen, and M. Shaposhnikov, Nucl. Phys. **B493**, 413 (1997).
[10] M. Reuter and C. Wetterich, Nucl. Phys. **B408**, 91 (1993).
[11] B. Bergerhoff and C. Wetterich, hep-ph/9508352; hep-ph/9611462.
[12] N. Tetradis, Nucl. Phys. **B488**, 92 (1997).
[13] W. Buchmüller and O. Philipsen, Nucl. Phys. **B443**, 47 (1995).
[14] K. Kajantie, M. Laine, K. Rummukainen, and M. Shaposhnikov, Phys. Rev. Lett. **77**, 2887 (1996).
[15] C. N. Yang and T. D. Lee, Phys. Rev. **87**, 404 (1952); **87**, 410 (1952); K. Huang, *Statistical Mechanics* (Wiley, New York 1987); M. E. Fisher, in *Lectures in Theoretical Physics* (University of Colorado Press, Boulder, CO, 1965), Vol. 7c.
[16] E. Marinari, *Optimized Monte Carlo Methods*, Lectures at the 1996 Budapest Summer School on Monte Carlo Methods, cond-mat/9612010.
[17] Y. Aoki, Nucl. Phys. B (Proc. Suppl.) **53**, 609 (1997); hep-lat/9612023.
[18] A. Ferrenberg and R. Swendsen, Phys. Rev. Lett. **61**, 2635 (1988); **63**, 1195 (1989).
[19] C. Borgs and R. Kotecký, J. Stat. Phys. **61**, 79 (1990); C. Borgs, R. Kotecký, and S. Miracle-Solé, *ibid.* **62**, 529 (1991).
[20] G. D. Moore, Nucl. Phys. **B493**, 439 (1997).
[21] B. Bunk, Nucl. Phys. B (Proc. Suppl.) **42**, 566 (1995).
[22] M. Laine, Phys. Lett. B **385**, 249 (1996).
[23] M. Gürtler, E.-M. Ilgenfritz, and A. Schiller, Z. Phys. C (to be published).